JACS
JOURNAL OF THE AMERICAN CHEMICAL SOCIETY

Article

pubs.acs.org/JACS

Complete Chemical Shift Assignment of the ssDNA in the Filamentous Bacteriophage fd Reports on Its Conformation and on Its Interface with the Capsid Shell

Omry Morag, Gili Abramov, and Amir Goldbourt*

School of Chemistry, Raymond and Beverly Sackler Faculty of Exact Sciences, Tel Aviv University, Ramat Aviv 69978, Tel Aviv, Israel

Supporting Information

ABSTRACT: The fd bacteriophage is a filamentous virus consisting of a circular single-stranded DNA (ssDNA) wrapped by thousands of copies of a major coat protein subunit (the capsid). The coat protein subunits are mostly α-helical and curved, and are arranged in the capsid in consecutive pentamers related by a translation along the main viral axis and a rotation of ~36° (C_5S_2 symmetry). The DNA is right-handed and helical, but information on its structure and on its interface with the capsid is incomplete. We present here an approach for assigning the DNA nucleotides and studying its interactions with the capsid by magic-angle spinning solid-state NMR. Capsid contacts with the ssDNA are obtained using a two-dimensional $^{13}C-^{13}C$ correlation experiment and a proton-mediated $^{31}P-^{13}C$ polarization transfer experiment, both acquired on an aromatic-unlabeled phage sample. Our results allow us to map the residues that face the interior of the capsid and to show that the ssDNA−capsid interactions are sustained mainly by electrostatic interactions between the positively charged lysine side chains and the phosphate backbone. The use of natural abundance aromatic amino acids in the growth media facilitated the complete assignment of the four nucleotides and the observation of internucleotide contacts. Using chemical shift analysis, our study shows that structural features of the deoxyribose carbons reporting on the sugar pucker are strikingly similar to those observed recently for the Pf1 phage. However, the ssDNA−protein interface is different, and chemical shift markers of base pairing are different. This experimental approach can be utilized in other filamentous and icosahedral bacteriophages, and also in other biomolecular complexes involving structurally and functionally important DNA−protein interactions.

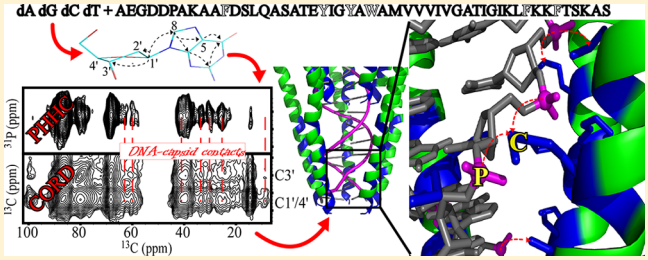

INTRODUCTION

The fd bacteriophage is a 16 megadalton filamentous virus having a diameter of ~7 nm and a length of ~1 μm. It consists of a circular single-stranded DNA (ssDNA) genome encapsulated in a capsid that contains almost exclusively several thousands of copies of structurally identical major coat protein subunits. The 50-residue-long major coat proteins constitute 85% of the virion mass, the genome 12%, and other minor coat proteins (gp3, gp6, gp7, gp9), which are functional during assembly and infection, comprise up to 3% of the total mass and are undetectable in most spectroscopic characterization methods.[1−3] Structural properties about the fd phage and about other closely related viruses (Ff phages: fd, M13, f1) including partial information on their symmetry, capsid packaging, and dynamics were obtained by a variety of biophysical techniques including X-ray fiber diffraction,[4−8] cryoEM studies,[9] static SSNMR,[8,10−12] magic-angle spinning (MAS) NMR,[13,14] and other spectroscopic methods.[2,15−17] It was shown that the protein subunits are mostly α-helical, curved, and are related by a 5-fold symmetry. Successive pentamers along the virion have an approximate or exact 2-fold screw axis (C_5S_2 − class-I symmetry), and hydrophobic interactions between subunits stabilize the capsid.[6,18,19]

The nucleobase composition[2] in wild-type fd is 25% adenine, 34% thymine, 21% guanine, and 20% cytosine. Circular dichroism spectroscopy suggests that the DNA in fd virus is organized in a right-handed helix with bases facing inward and phosphates facing outward.[20] Static SSNMR[11] and laser Raman[15,21] studies reported that the DNA phosphate backbone is highly disordered, and in a series of Raman studies it was proposed, on the basis of deoxyguanosine (dG, 21% of the genome) markers, that the sugar pucker is in a C3′-endo/*anti* conformation. Deoxythymidine (dT, 34%) markers were proposed to be either consistent with C3′-endo/*anti*[21,22] or C2′-endo/*anti*,[15] while markers of other nucleotides were obscured by the protein capsid resonances.

Despite extensive studies on filamentous phages, many features regarding the capsid and DNA conformation are in debate. For example, the interface between the DNA and the capsid shell has not been characterized, and different models of a mutant capsid suggest different protein subunit orientations; mutations of terminal lysine residues result in altered phage lengths,[23] but it is not clear whether electrostatic interactions

Received: May 12, 2013
Published: January 22, 2014

mediate the capsid−DNA interaction interface, as theoretically suggested for icosahedral RNA-viruses.[24] Also, MAS solid-state NMR studies on wild-type fd and the closely related M13 phage conducted by our group[13,14] point to a C2′-endo/C3′-exo conformation, unlike most Raman studies. Yet, these observations have been based on average deoxyribose sugars shifts observed in the NMR data.

MAS solid-state NMR has become a key tool for studying the structure and dynamics of biopolymers.[25−27] Near-complete resonance assignments and in some instances 3D structures have been reported for small and medium-sized globular proteins,[28−30] membrane proteins,[31−34] macromolecular assemblies,[35,36] amyloid fibrils,[37,38] and viruses.[35,39−44] MAS NMR studies also provide insight into structure and dynamics of poly nucleic acids[45−47] and were used to study protein−RNA interactions.[48−50] ^{31}P NMR was used to study oligonucleotides, phosphorylated amino acids, and membranes.[51−53]

While we focus here on a filamentous bacteriophage virus, interactions between proteins and DNA play both regulatory and functional roles in many cellular processes including DNA replication, restriction, recombination, gene expression, and transcription.[54] Nucleotide-specific chemical shift information can report on the conformation, dynamics, and molecular environment of the genome. In Pf1 phage, the unique ssDNA conformation was studied by utilizing dynamic nuclear polarization (DNP) experiments to obtain enhanced homonuclear ^{13}C−^{13}C correlations spectra.[40] In a series of studies on the 100 kDa $(CUG)_{97}$ RNA repeat polymer,[50,55,56] which utilized proton-mediated ^{13}C−^{13}C and ^{13}C−^{15}N correlations,[57,58] the type of hydrogen bonding and the existence of GC base pairing report on an A-form helix conformation with a C3′-endo sugar pucker and an anti glycosidic torsion angle χ. ^{31}P−^{15}N transferred echo double resonance (TEDOR) experiments allowed the measurements of distances between an RNA backbone and a ribonucleoprotein,[49] and ^{31}P−^{15}N rotational echo double resonance (REDOR) experiments were used to partially characterize protein−DNA interactions in the T4 icosahedral bacteriophage.[44]

In this study, we rely on several new experimental approaches to elucidate key structural properties of the circular ssDNA in intact wild-type fd bacteriophage, and characterize its interface with the protein capsid. These results, acquired due to the preparation of a unique aromatic-unlabeled phage sample suitable for DNA studies, are obtained from complete carbon assignments of the ssDNA, including nucleotide-specific ribose shifts, which facilitate the observation of interactions between the phosphates, sugars, and bases with the phage capsid. Consequently, we experimentally demonstrate that electrostatic interactions dominate the interface, and interface residues provide structure restraints on the coat protein orientation. In addition, analysis of the ssDNA shifts reports on its conformation, and comparison to the Pf1 virus clarifies key differences between these phage systems.

EXPERIMENTAL SECTION

Uniformly ^{13}C- and ^{15}N-Labeled fd Phage. The fd phage containing a wild-type capsid and an extended genome with a tetracycline resistance[59] was prepared, purified, characterized, and packed as previously described by Abramov et al.[14]

Aromatic Unlabeled ^{13}C/^{15}N-Labeled fd Phage. A sample of fd phage, labeled uniformly with ^{13}C and ^{15}N apart from the aromatic residues Trp, Phe, and Tyr (YFW^{unlab}-^{13}C/^{15}N-fd), was prepared by supplementing the minimal media, in addition to 4 g/L ^{13}C-glucose and 0.5 g/L $^{15}NH_4Cl$, with 0.2 g/L of natural abundance phenylalanine, tyrosine, and tryptophan. These concentrations were sufficient to block the production of these amino acids in the pentose phosphate pathway.[60] The aromatic unlabeled fd sample was purified, characterized, and packed as described for the fully labeled fd phage. Figure S1 in the Supporting Information shows the comparison of a 1D ^{13}C CPMAS spectra of the uniformly enriched and aromatic unlabeled samples. The elimination of all aromatic signals is clearly observed, revealing the underlying DNA signals.

NMR Experiments and Data Analysis. NMR data were collected on a Bruker Avance-III wide-bore 14.1 T solid-state NMR spectrometer. ^{13}C−^{13}C and ^{15}N−^{13}C correlation experiments were performed using a 4 mm Efree probe operating in ^{1}H−^{13}C−^{15}N mode. ^{31}P−^{13}C correlation experiments were performed using a 4 mm triple resonance DVT probe operating in ^{1}H−^{31}P−^{13}C mode. During all experiments, the sample temperature was set to −15 °C on the controller, which is approximately +10 °C after correcting for frictional heating.

^{13}C, ^{31}P, and ^{15}N magnetizations were prepared using power levels of 50 kHz during cross-polarization[61] (CP) and a 10% linearly ramped ^{1}H pulse set to the optimal (first) Harman−Hahn condition.[62] To avoid most of the overlap between the carbonyl first sideband and the DNA deoxyribose resonances, spinning speeds of 12 kHz were applied, unless stated otherwise. Proton decoupling of ∼80 kHz was applied using the swept-frequency two-pulse phase modulation technique (SW_f-TPPM).[63] ^{13}C−^{13}C magnetization transfer was accomplished using RF assisted diffusion[64] (RAD)/dipolar assisted rotational resonance[65] (DARR) with mixing times of 15, 100, and 250 ms and by using the supercycled combined $R2^{\nu}_{n}$-driven sequence[66] ($CORD_{xy4}$) with mixing times of 150 and 500 ms (CORD150 and CORD500). The radio frequency field strengths for these composite pulses during the mixing time on the ^{1}H channel were set to 12 kHz for $R2^{\nu}_{1}$ and 6 kHz for $R2^{\nu}_{2}$($\nu_{1H} = \nu_r$ and $\nu_{1H} = \nu_r/2$, respectively). ^{1}H−^{1}H mixing in the PHHC experiments was accomplished using proton driven spin diffusion[67] (PDSD) with a mixing time of 500 μs. Heteronuclear P−H and H−C CP contact times in the PHHC experiments were set to 1750 and 250 μs, respectively. Magnetization transfer between ^{15}N and ^{13}C in the 2D NCA experiment was acquired using the double cross-polarization scheme (DCP).[68] All acquisition and processing parameters can be found in Table S1 of the Supporting Information.

NMR data were processed using the NMRPipe[69] and Topspin 2.1 software packages, and subsequently analyzed using the program SPARKY.[70] The ^{13}C chemical shifts were referenced externally to the adamantane CH_2 peak at 40.48 ppm.[71] ^{15}N shifts were externally referenced to solid $^{15}NH_4Cl$ (39.27 ppm with respect to liquid ammonia at 25 °C[72]), and ^{31}P shifts were externally referenced to 85% (14.6 M) phosphoric acid at 0 ppm.[73]

RESULTS AND DISCUSSION

To unambiguously observe correlations between the DNA and the capsid shell, we initially assigned the DNA nucleotides, and consequently performed experiments that probe contacts between the shell and three elements of the nucleotides: the phosphate backbone, the deoxyribose moieties, and the bases.

Resonance Assignment of fd ssDNA. Nucleotide-specific assignments of DNA resonances using a uniformly ^{15}N/^{13}C labeled sample result in spectral overlap with the intense peaks of the coat protein aromatic side chains; hence many base resonances cannot be unambiguously assigned. To overcome this spectral congestion, we performed ^{13}C−^{13}C homonuclear correlation experiments using an fd sample, in which all carbons are labeled except those belonging to aromatic residues. The removal of the aromatic signals in a 1D ^{13}C CPMAS spectrum is clearly seen in Supporting Information Figure S1. The comparison between the fully labeled sample and the aromatic unlabeled sample reveals the signals of the DNA bases

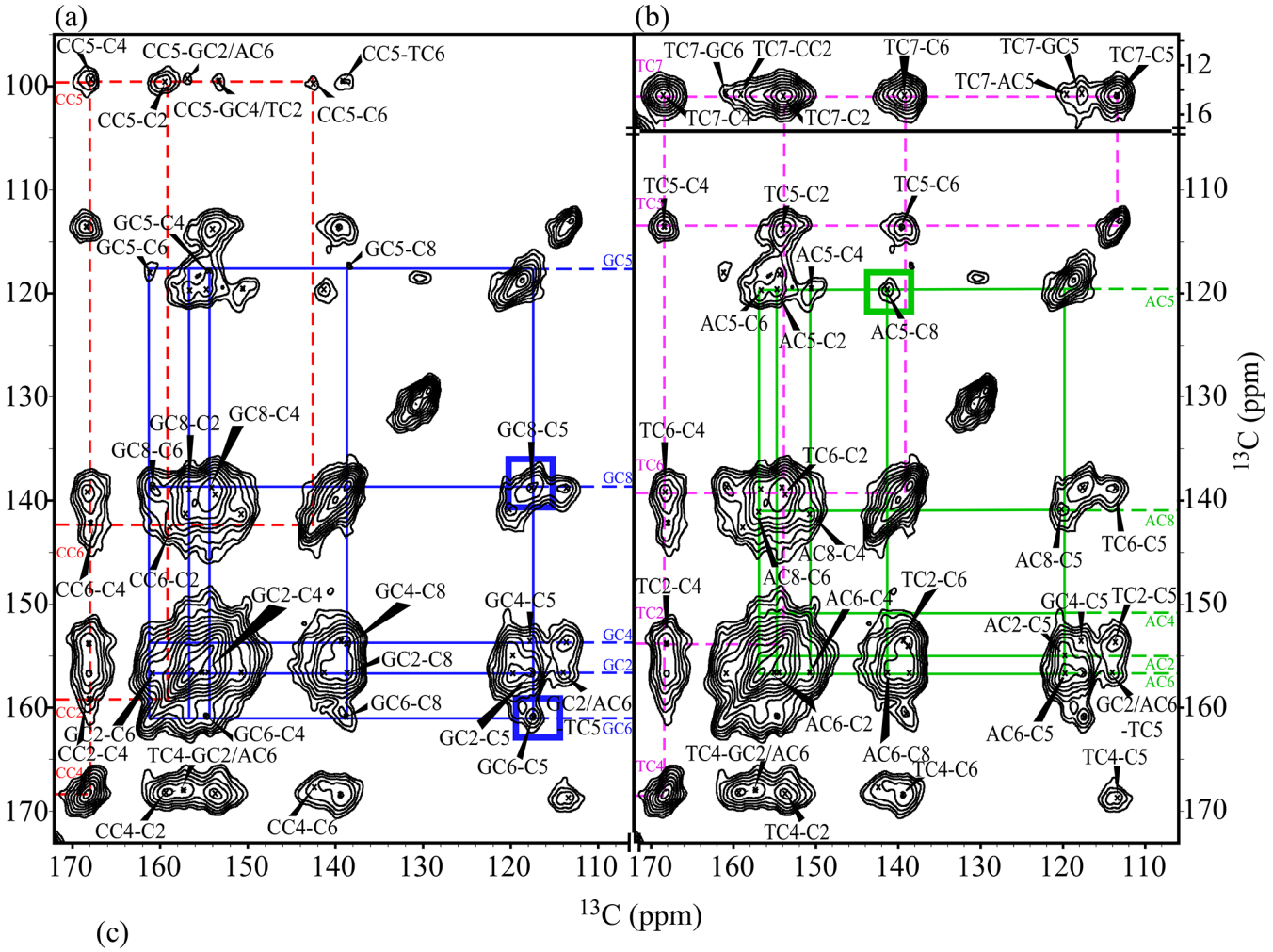

(c)

dG	C2	C4	C5	C6	C8
C2 (156.5)	■	⊗	×	×	×
C4 (154.0)	⊗	■	×	⊗	⊗
C5 (117.6)	⊗	×	■	×	×
C6 (161.0)	×	×	×	■	×
C8 (138.6)	×	⊗	×	×	■

dC	C2	C4	C5	C6
C2 (159.2)	■	⊗	×	⊗
C4 (168.0)	×	■	×	×
C5 (99.2)	×	×	■	×
C6 (142.4)	×	×	×	■

dA	C2	C4	C5	C6	C8
C2 (154.6)	■	O	×	⊗	O
C4 (150.6)	O	■	O	⊗	O
C5 (119.8)	×	×	■	×	×
C6 (157.0)	⊗	×	×	■	×
C8 (141.2)	⊗	×	×	⊗	■

dT	C2	C4	C5	C6	C7
C2 (153.4)	■	×	×	⊗	×
C4 (168.5)	×	■	×	×	×
C5 (113.6)	×	×	■	×	×
C6 (139.2)	⊗	×	×	■	×
C7 (14.4)	×	×	×	×	■

Figure 1. Nucleotide-specific assignments of base carbons in the ssDNA of fd phage. Extracted regions from a 2D ^{13}C–^{13}C CORD500 spectrum illustrating (a) assignments of dG and dC nucleotides; and (b) assignments of dA and dT nucleotides. The experiment was conducted on a YFW^{unlab}-^{13}C/^{15}N-fd sample and acquired with a spinning speed of 12 kHz. Solid blue and green lines (from both sides of the diagonal) show the nucleotide walks of dG and dA, respectively. Dashed red and magenta lines show the nucleotide walks of dC and dT, respectively. Circled cross-peaks served as the starting points for the assignments of dG and dA. (c) Assignment grids for each nucleotide illustrating the type of correlations observed in our spectrum: "×", resolved cross-peaks; "⊗", ambiguous cross-peaks; "O", missing cross-peaks. The rows present spins excited during t_1, and columns present the acquisition dimension. The spectrum was processed with exponential broadening (150 Hz-t_1, 150 Hz-t_2) and is plotted using 25 contour levels starting at 6σ (σ being the noise root-mean-square, determined by SPARKY) and using a multiplicity of 1.2. Additional parameters can be found in Table S1 in the Supporting Information.

underlying the capsid aromatic signal. In these experiments, and also in other 2D experiments, no loss of other signals was observed for other residues, indicating that no detectable scrambling occurs. Any labeled aromatic signals, if existing, are below the noise level and were unobserved as well.

To obtain the assignment of the DNA, we conducted the ^{13}C–^{13}C homonuclear supercycled CORD experiment, as it was recently shown to be an efficient, broadband, polarization transfer technique, and that it is well suited for resonances assignments and distance measurements of various biological systems.[66] Although CORD was developed for experiments performed at high spinning speeds, we show here very efficient polarization transfer for the DNA at a moderate spinning speed. Such transfer is essential because the bases contain mostly quaternary carbons that are not very efficiently polarized in the initial CP step. The full nucleotide-specific assignment list, appearing in Table S2 of the Supporting Information, was obtained using a "nucleotide-walk" along the spectra, obtained by analysis of intranucleotide cross-peaks, similarly to the "side-chain" walks for assigning amino acids. Anchor nuclei, which have well-resolved shifts or unique cross-peaks, were initially assigned using the chemical shift data in the BMRB[74] and by a

dx.doi.org/10.1021/ja412178n | J. Am. Chem. Soc. 2014, 136, 2292–2301

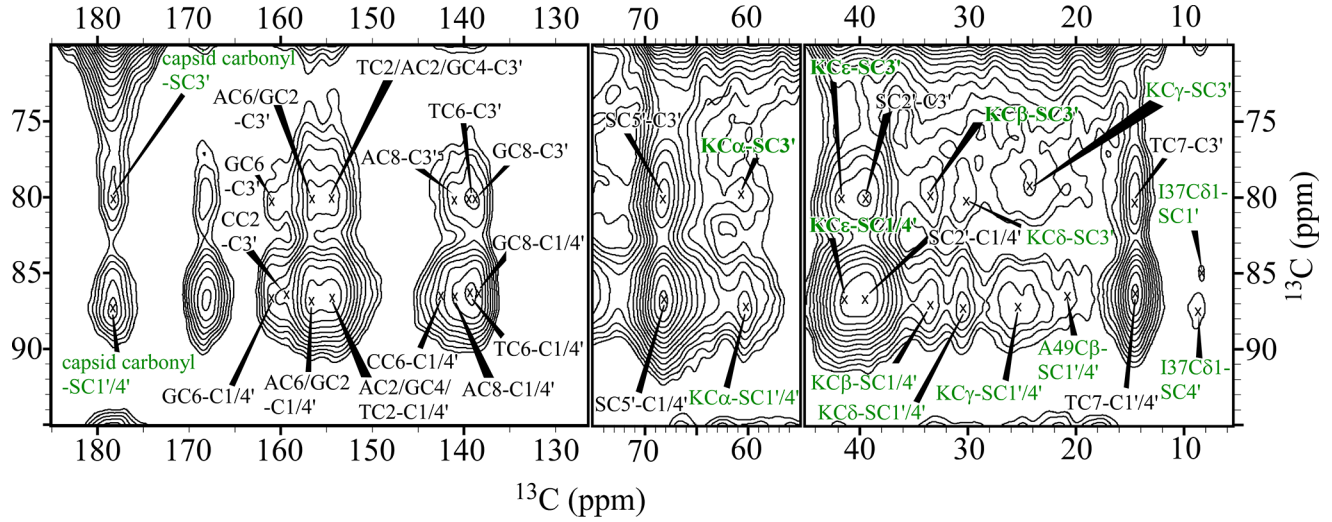

Figure 2. Sugar–capsid interactions. Extracted regions from a 2D ^{13}C–^{13}C CORD500 spectrum conducted on the YFW^{unlab}-^{13}C/^{15}N-fd sample showing the deoxyribose carbons C1′, C3′, C4′, and C5′. Sugar–sugar and base–sugar cross-peaks are labeled in black, and sugar–capsid cross-peaks are in green. Acquisition and processing parameters are as in Figure 1. The spectrum is plotted using 15 contour levels starting at 8σ and using a multiplicity of 1.2. The vertical chemical shift axis corresponds to the acquisition dimension. Additional parameters can be found in the Supporting Information.

list of B-DNA chemical shifts, which was compiled by Sergeyev et el.[40] The actual strategy for assigning the DNA signals appears below, and is shown in detail in Figure 1 ((a) for dC, dG; (b) for dT, dA). Figure 1c details schematically the spectra where we differentiate the existence of a resolved cross-peak ("×"), a nonresolved cross-peak ("⊗"), and a missing signal ("○").

The deoxythymidine nucleotide (dT) comprises 34% of the fd bacteriophage genome, its carbon resonances are the strongest, and in particular its methyl carbon TC7 (carbon-7 of deoxythymidine, 14.4 ppm) and the quaternary carbon TC5 (113.6 ppm) are unique and clearly resolved (the specific numbering of the deoxyribose and the four nucleotides can be found in Figure S2a of the Supporting Information). Cross-peaks of these carbons with all other dT base-carbons were observed and assigned (shown in Figure 1b and in the dT table in Figure 1c). dC base carbons were mainly assigned using their unambiguous cross-peaks with CC5 (99.2 ppm) and further completed from additional correlations. The assignment and the nucleotide walk appear in Figure 1a and in the dC table (Figure 1c). For dA and dG, the assignments were more challenging because no individual carbon has a unique chemical shift and most of them resonate at DNA-congested regions of the spectra. However, they have unique cross-peaks; the cross-peak at 161.0–117.6 ppm could only be assigned to GC6–C5 (Figure 1a). All other dG base carbons were assigned on the basis of their cross-peaks with GC5 and GC6 carbons and on their mutual correlations. Moreover, the cross-peak GC8–C5 has removed the ambiguities between GC8 and AC8 at 138.6 and 141.2 ppm, respectively (TC6 at 139.2 ppm, was previously assigned) and between AC5 and GC5 (119.8 and 117.6 ppm, respectively). AC4 (150.6 ppm) and AC5 were assigned via their mutual unique correlations with AC8 (Figure 1b). Consequently, AC2 and AC6 (154.6 and 157.0 ppm, respectively) were assigned via their contacts with AC5. We note that 58% (11/19) of the assigned carbons (mainly quaternary carbons) do not appear in the BMRB database, and therefore their assignments can be compared only to small molecules and to very few B-DNA studies of small DNA fragments (see Supporting Information Table S2). As a result of these assignments, we could assign internucleotide correlations (some examples are given in Figures 1 and 3, and a full list of internucleotide contacts appears in Supporting Information Table S3), suggesting base pairing and/or base stacking in the fd ssDNA.

The deoxyribose carbons were ambiguously assigned in our previous studies of the fd and M13 bacteriophage[13,14] and were based mostly on intra deoxyribose contacts, and on contacts with the dT methyl group. The new correlations observed here allow us to differentiate between sugar chemical shifts arising from different nucleotides (Figures 2 and 3 and Supporting Information Table S2). The many sugar–base correlations observed in our spectra also confirmed our assignments for the DNA bases and sugars.

The ssDNA chemical shifts were deposited in the BMRB, under accession number 19734.

ssDNA–Capsid Interactions. The DNA assignment obtained here and our previous capsid assignment of the phage[13,14] were used to identify unambiguous interactions between the DNA and the capsid. As the DNA molecule is composed of a nucleobase and a backbone made of alternating sugars and phosphate groups, better insight of the ssDNA–capsid interface can be achieved by analyzing the interactions between the capsid to the different parts of the DNA molecule. Therefore, the ssDNA–capsid interactions observed in all our spectra can be divided into three groups: sugar–capsid contacts, base–capsid contacts, and phosphate–capsid contacts.

Sugar–Capsid Interactions. One set of correlations between the DNA and the capsid was observed in the CORD500 spectral region belonging to the DNA sugars, shown in Figure 2. C2′ carbons have a shift (~40 ppm) that overlaps with the protein capsid and are not shown here. In addition to many DNA sugar–base correlations, we detected contacts between the sugars and carbonyl carbons (at ~178.3 ppm) that could only be assigned to the capsid and probably belong to amino acids in the C-terminus of the coat protein; however, these contacts are highly ambiguous. Non ambiguous

dx.doi.org/10.1021/ja412178n | J. Am. Chem. Soc. 2014, 136, 2292–2301

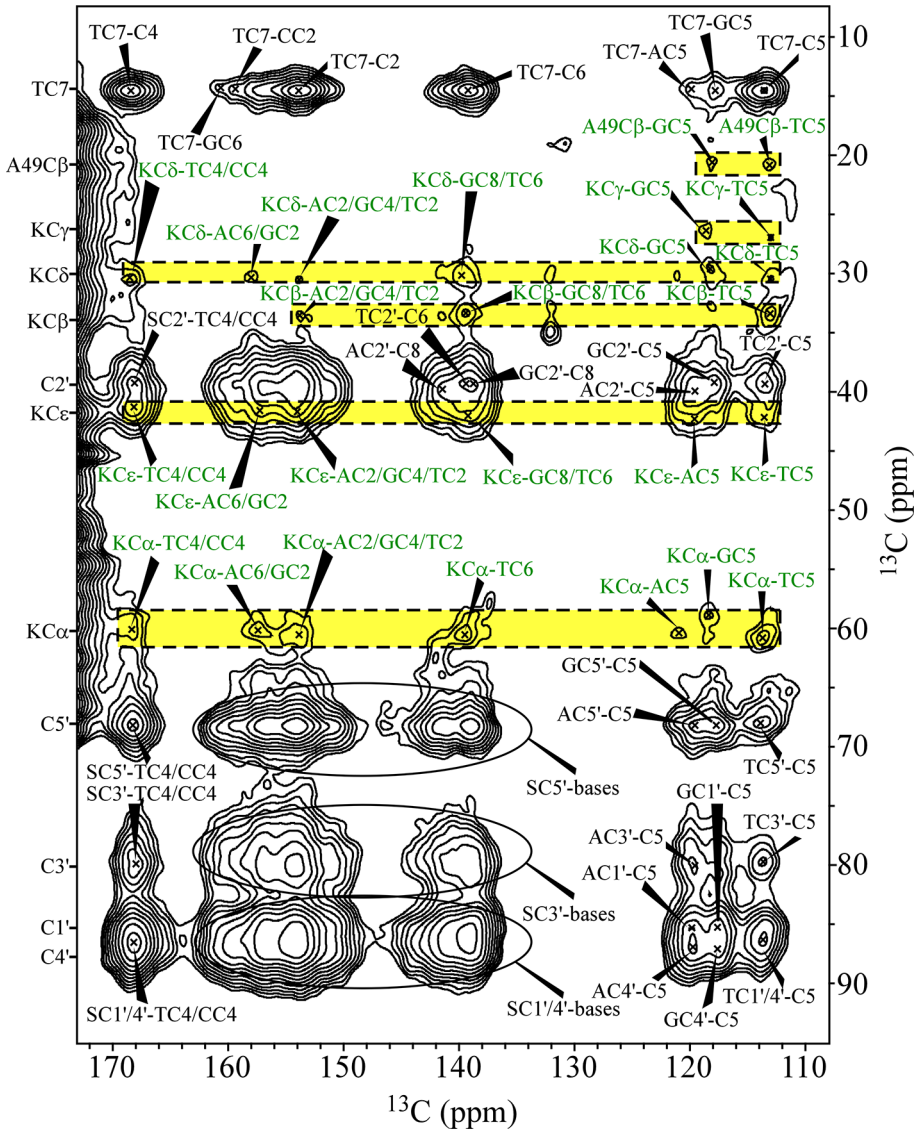

Figure 3. Base−capsid interactions. A portion from the 2D ^{13}C−^{13}C CORD500 spectrum conducted on the YFW^{unlab}-^{13}C/^{15}N-fd sample showing the different nucleobase carbons region. Sugar−base and base−base cross-peaks are labeled in black, and base−capsid cross-peaks are in green and highlighted. Acquisition and processing parameters are as in Figure 1.

contacts were observed between the DNA sugars and the capsid aliphatic carbons (e.g., A49Cβ, I37Cγ) and in particular between the sugar carbons and the entire Lys side chain carbons. Those are clearly indicated in Figure 2.

Base−Capsid Interactions. Correlations between the C-terminal residues of the capsid and carbons belonging to the different DNA bases were observed in our DARR250 and CORD500 spectra. Because the ssDNA in fd is circular with stacked bases pointing inward,[2,20] the bases are more distant from the capsid than the sugar moieties, and thus only weak signals are observed in the highlighted regions of Figure 3 (CORD500 spectrum). The majority of the base−capsid contacts are between carbons of different bases and the entire side-chain carbons of the C-terminal Lys residues. Single contacts between GC5 and TC5 to A49Cβ are also observed in this spectrum. These cross-peaks reflect the proximity of the ssDNA to the C-terminal region of the helical coat protein, report on the residues involved in the interface, and support the ultraviolet resonance Raman (UVRR) studies that showed that the thymine marker of packaged fd DNA may reflect interactions with the protein coat.[22]

Phosphate−Capsid Interactions. Correlations of the phosphate backbone with the ssDNA nucleosides or with side-chains of amino acids belonging to the coat protein can be probed using ^{31}P−^{13}C/^{15}N correlations. In Figure 4, we show the pulse sequence we have used to obtain such transfers. It is similar to the experiment proposed by Spiess[57] and later applied to protein assignment[58] and structure determination,[33] with the exception that one of the dimensions is replaced with ^{31}P (a homonuclear PHHP experiment was applied to study inorganic materials by Massiot et al.[75]). Because of the reduced spectral width of ^{31}P, and the enhanced spectral dispersion of the ^{13}C chemical shifts, we implemented the PHHC scheme rather than using ^{31}P detection corresponding to a CHHP scheme.

To validate the PHHC experiment, we applied it to *O*-phospho-L-serine as a model system. The signal intensity buildup curves of the P−Cα and P−Cβ correlations taken from 2D PHHC spectra are shown in Supporting Information Figure

dx.doi.org/10.1021/ja412178n | J. Am. Chem. Soc. 2014, 136, 2292−2301

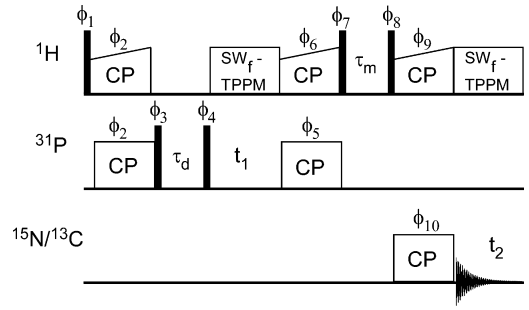

Figure 4. Pulse sequence for the *z*-filtered PHHC experiment (adapted from Lange et al.[58]). Filled rectangular pulses represent 90° pulses. In a different version, the ^{31}P and ^{13}C channels can be exchanged, and the ^{13}C channel can be replaced with a ^{15}N channel making it a N/CHHP correlation experiment (or PHHN). The phase cycle was as follows: $\phi_1 = 1_{16}3_{16}$, $\phi_2 = 0$, $\phi_3 = 1$, $\phi_4 = 31$, $\phi_5 = 0$, $\phi_6 =$ 0011 2233, $\phi_7 =$ 0011 2233, $\phi_8 =$ 3300 1122 1122 3300, $\phi_9 =$ 0011 2233, $\phi_{10} =$ 0011 2233, and $\phi_{rec} =$ 0213 2031 2031 0213 2031 0213 0213 2031. The phase ϕ_4 was incremented according to the States-TPPI scheme[76] to obtain phase-sensitive detection in the indirect t_1 dimension. The phase values are multiples of 90°.

S3. A slower build-up rate of the Cα carbon clearly indicates that the signal intensity of the ^{13}C spins is dependent on their distance from the phosphate group (crystal structure:[77] P−Cα, 2.2 Å; P−Cβ, 1.4 Å). Another interesting observation is that maximal Cβ intensity is obtained almost instantly. This is a result of the initial ^{31}P−^{1}H cross-polarization step of 1.75 ms, which transfers magnetization directly to the protons attached to Cβ. This long ^{31}P−^{1}H transfer time was used to mimic the DNA phosphate backbone, which lacks protons.

2D PHHC experiments were conducted on our aromatic unlabeled sample (Figure 5). Clear and intense sugar signals

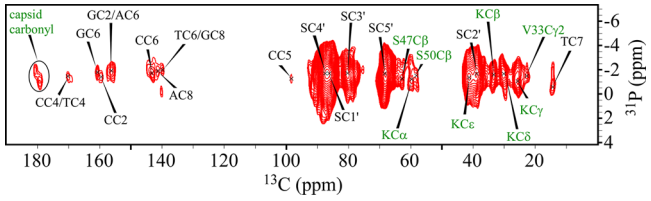

Figure 5. 2D PHHC spectrum of the YFW^{unlab}-^{13}C/^{15}N-fd sample. The experiment was performed using a spinning speed of 12 kHz and a proton mixing time of 500 μs. A total experimental time of 117 h was used to collect the 2D data corresponding to acquisition times of 2.5 ms (30 increments) and 29 ms in indirect and acquisition dimensions, respectively. Processing parameters are similar to those in Figure 1. Fifteen contour levels are plotted starting at 6σ and using a multiplicity of 1.1.

were observed including all resonances from C1′−C5′, indicating that a direct transfer from the phosphates to the sugar protons occurred. In addition, several phosphate−base correlations were observed. These signals have lower intensities as expected, because the bases are more distant from the phosphate group than the ribose part. We also observed signals that clearly belong to the coat protein. In particular, a very intense LysCε (at ∼42 ppm) signal appears in this spectrum, suggesting a very close vicinity to the phosphates, similarly to the sugar signals. Weak signals at ∼179.3 ppm were also detected that can be assigned only to the capsid carbonyl carbons. Such correlations were also observed with the sugar signals. Additional contacts to the capsid are observed with aliphatic carbons at 20−70 ppm (with the exception of the sugar C2′ carbons at ∼38.5 ppm) and report on contacts to the entire lysine side chain, and on contacts to additional residues facing the DNA including terminal serines (S47, S50) and Cγ of V33.

The strongest reporters of the interface between the ssDNA and the protein capsid are the signals associated with the positively charged side chains of the C-terminal Lysine residues (40, 43, 44, 48) and, in particular, the closest ε-carbon. According to their assignments,[14] Cε signals resonate at frequencies of 41.0−42.5 ppm. These values have some small overlap with the deoxyribose C2′ carbons (38.3−41.2 ppm); however, the spectral overlay shown in Figure 6 demonstrates

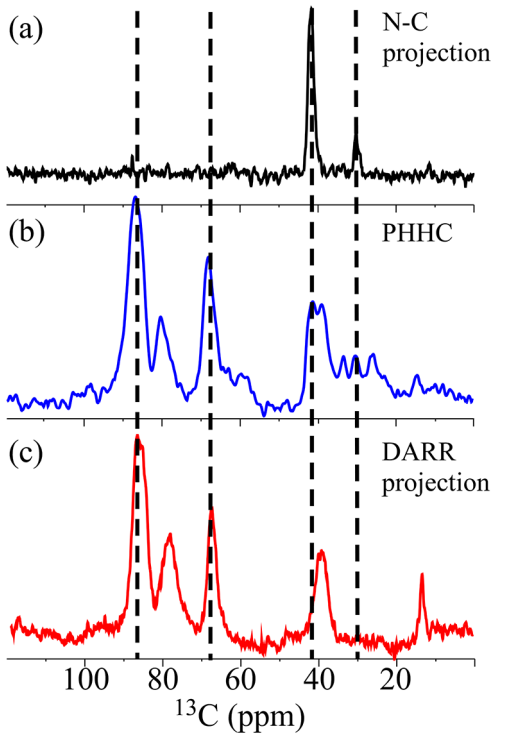

Figure 6. Comparison of (a) summation of slices (31−39 ppm) from a NCA double-CP experiment taken around the chemical shift of lysine-Nζ, and showing correlations with Cε (left signal) and Cδ carbons; (b) summation of slices (−4 to 1 ppm) along the ^{31}P dimension from the PHHC experiment conducted on the YFW^{unlab}-^{13}C/^{15}N-fd sample and acquired with a proton mixing time of 500 μs; and (c) summation of slices belonging to the DNA sugar region (C1′/C4′, rows 80−90 ppm) from a DARR100 experiment. The dashed lines indicate the positions (from left to right) of C1′/C4′ (which are unresolved), C3′, KCε, and KCδ.

clearly that in the PHHC experiment, Cε is polarized with magnetization originating from the phosphate backbone. The top spectrum (Figure 6a) shows slices from an NCA experiment, which correspond to lysine-Nζ/Cε cross-peaks, and these signals are centenred around 41.8 ppm. This shift matches the low-field peak of the PHHC split signal in the same region (Figure 6b, indicated by the dashed line), but has a higher frequency than the summation of sugar slices from the 2D ^{13}C−^{13}C DARR100 spectrum (rows 80−90 ppm), which are centered just below 40 ppm (Figure 6c). The PHHC signal therefore embeds both lysine−Cε and sugar−C2′ signals. Additional signals corresponding to the Lys side chain can also be identified (noted in Figure 5), supporting the observation of

dx.doi.org/10.1021/ja412178n | J. Am. Chem. Soc. 2014, 136, 2292−2301

an electrostatic phosphate−lysine interface. Further enlargement of the region between 38 and 43 ppm in the PHHC experiment appears in the Supporting Information (Figure S4).

Putting together the interactions observed in the CORD, DARR, and PHHC spectra, 56 contacts between the ssDNA and the capsid of the fd bacteriophage were assigned (see Supporting Information Table S4). The C-terminal residues of the capsid subunits, including the entire side chain of the lysines, interact with all of the DNA components: the phosphate groups, the sugar rings, and the four different nucleobases. The interface between the ssDNA and the capsid involves residues Val33, Ile37, Lys40, Lys43, Lys44, Ser47, Lys48, Ala49, and Ser50. While a significant outward kink in the helix was reported to appear at residue Ile39,[10] the side chain of Val33 still reaches the vicinity of the DNA. In the best structure currently available, that of the fd-Y21M mutant,[8] the N-terminal part of each subunit belonging to a certain pentamer (i.e., subunits *j*, *j*+1, ...*j*+4) and the C-terminal edge of the pentamer located right above it (subunits j+10, *j*+11, ...*j*+14) are in close contact up to around residue Val29 (see also Figure 7). Therefore, vertically adjacent pentamers do not hamper the interactions of Val33 and Ile37 with the DNA, as we observe in our spectra.

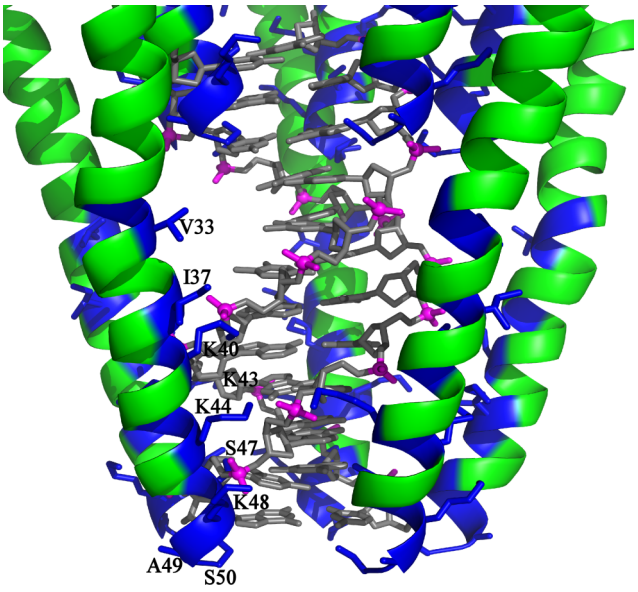

Figure 7. An illustration of the ssDNA−capsid interface in fd bacteriophage. A cartoon view of 10 major coat protein subunits (subunits *j*→*j*+4 and the C-terminal edge of *j*+10→*j*+14) was generated by PyMOL using the coordinates of the entry 2C0X. The pentamer containing the five subunits *j*+5→*j*+9 was omitted for clarity and undergoes similar interactions with another pentamer above it. A sticks representation of an encapsulated B-DNA was generated using the coordinates of entry 1BNA and inserted into the hollow capsid for illustrative purposes. The capsid residues that interact with the DNA (colored in blue) all point inward. The phosphate moieties are emphasized and colored in magenta.

ssDNA Conformation. Nucleotide chemical shifts are influenced by the deoxyribose conformation, hydrogen bonding (base pairing), and base stacking, and are also reporters of the glycosidic DNA-backbone torsion angle χ.[78−84] Because the fd genome is extensively large, the chemical shifts we observe are averaged over many sites, and therefore neighboring-residue effects[85] are insignificant. We analyzed the chemical shifts observed in our spectra and compared them to DNA average shifts published in the BMRB, to small molecules, and to those of B-DNA. Our experimental chemical shifts of fd, tabulated in the Supporting Information (Table S2), are also compared to those measured for Pf1, a phage for which a unique DNA conformation was proposed.[92] We note here that for several bases only very few reports of quaternary carbons have been found for B-DNA (the actual number appears in the Supporting Information) and none in the BMRB, and therefore interpretation of small shift deviations for these carbons has not been attempted, or is treated with great caution.

We have shown before, and confirmed here in a nucleotide-specific ribose assignments, that on the basis of experiments and calculations performed by Santos et al.[84] and others,[86] the deoxyribose shifts are consistent with the closely related C2′-endo or C3′-exo sugar puckers (S-type). The C3′-endo conformation was discarded due to the significantly high frequency shifts of C3′ (∼80 ppm) and C5′ (∼68 ppm). Interestingly, this result is not consistent with former Raman studies based on mainly dG but to some extent also dT markers that support C3′-endo/*anti* conformation;[21,22] however, ssNMR data of sugar resonances are almost identical for fd and Pf1, and the Raman data of the latter indicated C2′-endo/*anti* conformation.[21] Differentiation between the 3′-exo and 2′-endo is more dependent[84] on C2′ (42 ppm vs 38.2 ppm, respectively), C4′ (88.4 ppm vs 84.5 ppm), and to some extent C5′ (67.1 ppm vs 65.7 ppm) with consistently higher shifts for the 3′-exo conformation. The corresponding shifts in fd average 40, 87, and 68 ppm and lie between the values of these two conformations. With current data, we cannot therefore determine whether those values indicate a distribution of the two pucker conformations or are a result of the unique circular ssDNA structure. Nevertheless, on the basis of these values,[87] we can assume that the S-type pucker has a gauche (γ) conformation.

The glycosidic torsion angle χ is an important parameter in determining the conformation of the DNA. It is defined by the atoms O4′−C1′−N9−C4 for purine bases (dG, dA) and O4′−C1′−N1−C2 for pyrimidine bases (dT, dC) and therefore determines the orientation of the bases with respect to the sugars. While the purines can exist in *anti* (∼ −120°) or *syn* (∼60°) conformations (see Figure S2b in the Supporting Information), pyrimidines can only adopt the *anti* conformation due to steric effects between the ribose and C2 carbonyl group. The χ angle is predicted from our data by analysis of the chemical shifts of the bases and to a smaller extent those of the deoxyribose shifts. Although trends in the sugar pucker and backbone sugar conformation have a much larger effect on their values, the similarity of dA and dG shifts to those of dC and dT and also the lack of significant upfield shift of C2′[80] may suggest an *anti* conformation. This conclusion is further supported by the slightly below average shift of AC8 (141.2 ppm in fd, −0.5 ppm from average of 84 entries in the BMRB/+0.5 ppm from 19 entries of B-DNA/smaller than random-coil shifts[85]), and the average shift of GC8 (138.6 ppm, +0.0 ppm, 91 entries/+0.6 ppm, 18 entries).[80−83] GC5 (117.6 ppm in fd) and AC5 (119.8 ppm) are also reporters of χ; however, calculations suggest that additional effects such as base pairing and stacking also affect their chemical shifts,[82,88] and in addition database information is scarce. Therefore, interpretation of their shift should be taken with care. Overall, our data point to an *anti* conformation for the glycosidic torsion angle in the fd

bacteriophage ssDNA, in agreement with previous Raman studies.[15,21,22]

According to several reports,[78,82,88,89] the most sensitive indicators of base pairing are TC4, GC2, and GC6, all of which shift to higher fields upon disruption of the hydrogen bonds. In fd, TC4 (which is very different from Pf1, see below) has a higher than average shift (+1.7 ppm from B-DNA but only four entries), and both GC2 and GC6 have average B-DNA values. To a smaller extent, lower shifts of CC6 observed in our spectra (−1.1 ppm from BMRB average) are also suggestive of hydrogen bonding.[78] While we assume and observe (from many internucleotide cross-peaks, see Figures 1 and 3 and Supporting Information Table S3) that hydrogen bonds should exist in the circular ssDNA of fd, these should be irregular or of different types, because Watson−Crick base pairing can only occur statistically in the phage.

Comparison to Pf1 Phage. The Pf1 phage, much like other virions, has a filamentous structure with a diameter of ∼7 nm. Its capsid also consists of many small-sized, α-helical subunits that package a similarly large genome[2] (∼7400 nucleotides); however, Pf1 is longer (∼1915 nm vs 880 nm of wild-type fd and ∼1300 nm of our antibiotic-resistant fth1 construct of fd). The length of Pf1 results from its unique nucleotide to subunit ratio of one, which differs from fd and other phages having a noninteger ratio larger than two.[1,2,90] The capsid of Pf1 adopts a helical symmetry (class-II) rather than the C_5S_2 symmetry of the fd phage. Its unique nucleotide to subunit ratio has been related to an unusual, stretched conformation of the packed circular single-stranded DNA.[91,92] A comparison between the fd and Pf1 phages using UVRR spectroscopy has shown fundamental differences in the organizations of the ssDNA molecule.[93] Base stacking was shown to be minimal as compared to fd, and the sugar ring conformation (dG and to some extent dT markers), as mentioned above, was found (unlike our ssNMR data) to adopt a C3′-endo/*anti* conformation for fd, and a C2′-endo/*anti* conformation for Pf1. 1D and 2D static SSNMR studies on oriented Pf1 and fd have shown that the DNA backbone structure of fd is disordered while that of Pf1 is well ordered.[11] The different modes of organizations of the viral genomes with respect to the capsid may also reflect a change in the DNA−capsid interface for fd and Pf1. In light of the recent NMR studies of the DNA in Pf1, and the current study, it is interesting to compare both the chemical shifts and the DNA−capsid interface of the two phages.

In Pf1, it was proposed that each aromatic tyrosine-40 residue stacks with a single nucleotide base[94,40] and that the interactions of positively charged side chains with the phosphate backbone are mediated by water molecules.[95] In fd, the ssDNA bases are most probably stacked similarly to a double-helix DNA, and the aromatic residues are involved in hydrophobic intersubunit interactions.[6,8,18] In fact, we could detect intersubunit interactions between the aromatic residues of the capsid protein (not shown) supporting former studies, and, unlike in Pf1, we cannot detect unambiguously aromatic-base correlations such as those observed for Pf1-Y40. As shown above, our experiments show that the main interactions are those of the lysine side chains with the phosphate backbone, and report on residues in the vicinity of the DNA. Indeed in fd there are four positively charged lysine residues in the C-terminus in comparison to only two (lysine and arginine) in Pf1.

It is also interesting to look for significant differences and similarities in the chemical shifts (Supporting Information, Table S2). Comparison of the sugar chemical shifts shows very similar shifts for C3′ and C5′, the principal reporters of the sugar pucker, similar C2′ shift, and slightly lower Pf1 minimal shifts for C1′ and C4′ carbons; however, they are not sufficiently resolved. Overlay of the $^{13}C-^{13}C$ homonuclear spectra of the two phages shows an almost identical spectrum in the deoxyribose region (not shown). It is therefore highly probable that the two phages adopt a similar puckering conformation.

In both viruses, most chemical shift data are consistent with an *anti* conformation, with GC8 in Pf1 taking a significant lower shift by over 2 ppm. Our results also show that AC2, AC4, and TC4 have a much smaller shift (∼2 ppm) than the Pf1 measurement, and AC6 and GC2 have slightly higher shifts in fd. These five shift changes are all consistent[78,88] with the existence of more hydrogen bonding in fd than in Pf1 regardless of the low counts for most of them in the database (only AC2 has a significant amount of data).

SUMMARY AND CONCLUSIONS

Determination of all carbon chemical shifts in the ssDNA molecule of the intact, wild-type fd phage allowed us to explore the ssDNA−capsid interface of this virus. In particular, many bases shifts of quaternary carbons, which are rarely present in the databases, have been assigned. The interface includes C-terminal residues that point toward the DNA, and, in particular, strong electrostatic interactions between the positively charged lysine side chains and the negatively charged DNA phosphate groups are observed. Contacts have been obtained using the assignment of DNA resonances, combined with our previous assignment of the fd capsid and with $^{31}P-^{13}C$ heteronuclear PHHC correlations. DNA assignments have been obtained by using $^{13}C-^{13}C$ homonuclear CORD and DARR magic-angle spinning solid-state NMR correlation experiments. We showed that in order to study the DNA of such systems a special labeling scheme is required, in which the sample is fully labeled while the aromatic residues are selectively unlabeled. Such a sample shows resolved signals for the different DNA base carbons due to the removal of aromatic signals.

Figure 7 illustrates a side view of the fiber-diffraction/static SSNMR model of fd-Y21M mutant bacteriophage (PDB: 2C0X[8]) with a B-DNA (PDB: 1BNA) molecule inserted in the center. The capsid residues that are involved in the circular ssDNA−capsid interface are colored in blue. The end of this interface (Val33) is also very close to the location of the second next pentamer, which interacts with the DNA in a similar fashion.

Structural properties were in part predicted from the chemical shifts of the nucleotides, and from cross-peak correlations. These shifts are consistent with an S-type/gauche sugar pucker conformation, an *anti* glycosidic torsion angle, and point to the existence of base pairing and base stacking. Comparison to Pf1 phage reveals similar deoxyribose spectra suggesting a similar sugar conformation, yet a much larger tendency for base pairing, and a different ssDNA−capsid interface.

This study provides an important step toward quantitative mapping of the ssDNA−capsid interface in the bacteriophage fd and therefore toward an atomic-level structure-determination of the entire phage. The approach for studying DNA in such systems and probing the interface with the capsid using unique

sample labeling and PHHC experiments is generally applicable also to other similar systems, in which DNA−protein interactions play an important structural and functional role.

■ ASSOCIATED CONTENT

Supporting Information

Experimental details, 1D ^{13}C CPMAS spectrum of the aromatic unlabeled sample, table of nucleotide assignments and comparison to other database and literature information, the four nucleotides and their numbering, sugar pucker and glycosidic angle cartoons, a table of internucleotide cross-peaks, PHHC experiments on a model system (*O*-phospho-L-serine), expansion of Figure 6, and a table of all DNA−capsid interactions. This material is available free of charge via the Internet at http://pubs.acs.org.

■ AUTHOR INFORMATION

Corresponding Author

amirgo@post.tau.ac.il

Notes

The authors declare no competing financial interest.

■ ACKNOWLEDGMENTS

Financial support was provided by the Israel Science Foundation. Support for the spectrometer was given in part by the center for Nanoscience and Nanotechnology of Tel Aviv University. The fth1 vector was a kind gift from Prof. Jonathan Gershoni from the Department of Cell Research and Immunology, Faculty of Life Sciences, Tel Aviv University. We would like to thank Prof. Loren Day for his long-term guidance on filamentous phage.

■ REFERENCES

(1) Day, L. A. In *Encyclopedia of Virology*, 3rd ed.; Allan, G., Webster, R., Eds.; Elsevier: Oxford, 2008; Vol. *1*, pp 117−124.
(2) Day, L. A.; Marzec, C. J.; Reisberg, S. A.; Casadevall, A. *Annu. Rev. Biophys. Biophys. Chem.* **1988**, *17*, 509−539.
(3) Marvin, D. A. *Curr. Opin. Struct. Biol.* **1998**, *8*, 150−8.
(4) Banner, D. W.; Nave, C.; Marvin, D. A. *Nature* **1981**, *289*, 814−816.
(5) Caspar, D. L.; Makowski, L. *J. Mol. Biol.* **1981**, *145*, 611−7.
(6) Marvin, D. A.; Hale, R. D.; Nave, C.; Helmer-Citterich, M. *J. Mol. Biol.* **1994**, *235*, 260−86.
(7) Marvin, D. A. *J. Mol. Biol.* **1966**, *15*, 8−17.
(8) Marvin, D. A.; Welsh, L. C.; Symmons, M. F.; Scott, W. R. P.; Straus, S. K. *J. Mol. Biol.* **2006**, *355*, 294−309.
(9) Wang, Y. A.; Yu, X.; Overman, S.; Tsuboi, M.; Thomas, G. J.; Egelman, E. H. *J. Mol. Biol.* **2006**, *361*, 209−15.
(10) Zeri, A. C.; Mesleh, M. F.; Nevzorov, A. A.; Opella, S. J. *Proc. Natl. Acad. Sci. U.S.A.* **2003**, *100*, 6458−6463.
(11) Cross, T. A.; Tsang, P.; Opella, S. J. *Biochemistry* **1983**, *22*, 721−726.
(12) Colnago, L. A.; Valentine, K. G.; Opella, S. J. *Biochemistry* **1987**, *26*, 847−54.
(13) Morag, O.; Abramov, G.; Goldbourt, A. *J. Phys. Chem. B* **2011**, *115*, 15370−15379.
(14) Abramov, G.; Morag, O.; Goldbourt, A. *J. Phys. Chem. B* **2011**, *115*, 9671−9680.
(15) Aubrey, K. L.; Thomas, G. J. *Biophys. J.* **1991**, *60*, 1337−49.
(16) Overman, S. A.; Kristensen, D. M.; Bondre, P.; Hewitt, B.; Thomas, G. J. *Biochemistry* **2004**, *43*, 13129−13136.
(17) Day, L. A. *J. Mol. Biol.* **1969**, *39*, 265−77.
(18) Overman, S. A.; Thomas, G. J. *Biochemistry* **1995**, *34*, 5440−5451.
(19) Arnold, G. E.; Day, L. A.; Dunker, A. K. *Biochemistry* **1992**, *31*, 7948−7956.
(20) Casadevall, A.; Day, L. A. *Biochemistry* **1983**, *22*, 4831−4842.
(21) Thomas, G. J.; Prescott, B.; Opella, S. J.; Day, L. A. *Biochemistry* **1988**, *27*, 4350−7.
(22) Wen, Z. Q.; Overman, S. A.; Thomas, G. J. *Biochemistry* **1997**, *36*, 7810−7820.
(23) Hunter, G. J.; Rowitch, D. H.; Perham, R. N. *Nature* **1987**, *327*, 252−4.
(24) Belyi, V. A.; Muthukumar, M. *Proc. Natl. Acad. Sci. U.S.A.* **2006**, *103*, 17174−8.
(25) Goldbourt, A. *Curr. Opin. Biotechnol.* **2013**, *24*, 705−715.
(26) McDermott, A.; Polenova, T. *Curr. Opin. Struct. Biol.* **2007**, *17*, 617−622.
(27) Shi, L.; Ladizhansky, V. *Methods Mol. Biol.* **2012**, *895*, 153−65.
(28) Knight, M. J.; Pell, A. J.; Bertini, I.; Felli, I. C.; Gonnelli, L.; Pierattelli, R.; Herrmann, T.; Emsley, L.; Pintacuda, G. *Proc. Natl. Acad. Sci. U.S.A.* **2012**, *109*, 11095−100.
(29) Zhou, D. H.; Shea, J. J.; Nieuwkoop, A. J.; Franks, W. T.; Wylie, B. J.; Mullen, C.; Sandoz, D.; Rienstra, C. M. *Angew. Chem., Int. Ed.* **2007**, *46*, 8380−3.
(30) Castellani, F.; van Rossum, B.; Diehl, A.; Schubert, M.; Rehbein, K.; Oschkinat, H. *Nature* **2002**, *420*, 98−102.
(31) Shahid, S. a; Markovic, S.; Linke, D.; van Rossum, B. J. *Nature* **2012**, *2*, 803.
(32) Cady, S. D.; Schmidt-Rohr, K.; Wang, J.; Soto, C. S.; Degrado, W. F.; Hong, M. *Nature* **2010**, *463*, 689−92.
(33) Lange, A.; Giller, K.; Hornig, S.; Martin-Eauclaire, M. F.; Pongs, O.; Becker, S.; Baldus, M. *Nature* **2006**, *440*, 959−962.
(34) Shi, L.; Lake, E. M. R.; Ahmed, M. A. M.; Brown, L. S.; Ladizhansky, V. *Biochim. Biophys. Acta, Biomembr.* **2009**, *1788*, 2563−2574.
(35) Goldbourt, A.; Gross, B. J.; Day, L. A.; McDermott, A. E. *J. Am. Chem. Soc.* **2007**, *129*, 2338−2344.
(36) Loquet, A.; Sgourakis, N. G.; Gupta, R.; Giller, K.; Riedel, D.; Goosmann, C.; Griesinger, C.; Kolbe, M.; Baker, D.; Becker, S.; Lange, A. *Nature* **2012**, *486*, 276−282.
(37) Tycko, R. *Annu. Rev. Phys. Chem.* **2011**, *62*, 279−99.
(38) Van Melckebeke, H.; Wasmer, C.; Lange, A.; Ab, E.; Loquet, A.; Böckmann, A.; Meier, B. H. *J. Am. Chem. Soc.* **2010**, *132*, 13765−75.
(39) Goldbourt, A.; Day, L. A.; McDermott, A. E. *J. Biol. Chem.* **2010**, *285*, 37051−37059.
(40) Sergeyev, I. V; Day, L. A.; Goldbourt, A.; McDermott, A. E. *J. Am. Chem. Soc.* **2011**, *133*, 20208−20217.
(41) Han, Y.; Ahn, J.; Concel, J.; Byeon, I.-J. L.; Gronenborn, A. M.; Yang, J.; Polenova, T. *J. Am. Chem. Soc.* **2010**, *132*, 1976−87.
(42) Byeon, I. J. L.; Hou, G.; Han, Y.; Suiter, C. L.; Ahn, J.; Jung, J.; Byeon, C.-H.; Gronenborn, A. M.; Polenova, T. *J. Am. Chem. Soc.* **2012**, *134*, 6455−66.
(43) Chen, B.; Tycko, R. *Protein Sci.* **2010**, *19*, 716−730.
(44) Yu, T. Y.; Schaefer, J. *J. Mol. Biol.* **2008**, *382*, 1031−42.
(45) Pederson, K.; Meints, G. A.; Shajani, Z.; Miller, P. A.; Drobny, G. P. *J. Am. Chem. Soc.* **2008**, *130*, 9072−9.
(46) Echodu, D.; Goobes, G.; Shajani, Z.; Pederson, K.; Meints, G.; Varani, G.; Drobny, G. *J. Phys. Chem. B* **2008**, *112*, 13934−44.
(47) Robinson, B. H.; Mailer, C.; Drobny, G. *Annu. Rev. Biophys. Biomol. Struct.* **1997**, *26*, 629−58.
(48) Huang, W.; Varani, G.; Drobny, G. P. *J. Biomol. NMR* **2011**, *51*, 347−56.
(49) Jehle, S.; Falb, M.; Kirkpatrick, J. P.; Oschkinat, H.; van Rossum, B. J.; Althoff, G.; Carlomagno, T. *J. Am. Chem. Soc.* **2010**, *132*, 3842−6.
(50) Asami, S.; Rakwalska-Bange, M.; Carlomagno, T.; Reif, B. *Angew. Chem., Int. Ed.* **2013**, *52*, 2345−2349.
(51) Dam, L.; Van Levitt, M. H. *J. Mol. Biol.* **2000**, *304*, 541−561.
(52) Stumber, M.; Geyer, M.; Graf, R.; Robert Kalbitzer, H.; Scheffzek, K.; Haeberlen, U. *J. Mol. Biol.* **2002**, *323*, 899−907.
(53) Magusin, P. C.; Hemminga, M. A. *Biophys. J.* **1995**, *68*, 1128−36.

(54) Voet, D.; Voet, J. G. In *Biochemistry*, 3rd ed.; Harris, D., Patrick, F., Eds.; John Wiley & Sons: Hoboken, NJ, 2004.
(55) Riedel, K.; Herbst, C.; Häfner, S.; Leppert, J. J.; Ohlenschläger, O.; Swanson, M. S.; Görlach, M.; Ramachandran, R.; Haefner, S.; Ohlenschlaeger, O.; Goerlach, M. *Angew. Chem., Int. Ed.* **2006**, *45*, 5620−5623.
(56) Riedel, K.; Leppert, J.; Ohlenschlager, O.; Gorlach, M.; Ramachandran, R. *J. Biomol. NMR* **2005**, *31*, 331−336.
(57) Wilhelm, M.; Feng, H.; Tracht, U.; Spiess, H. W. *J. Magn. Reson.* **1998**, *134*, 255−60.
(58) Lange, A.; Luca, S.; Baldus, M. *J. Am. Chem. Soc.* **2002**, *124*, 9704−9705.
(59) Enshell-Seijffers, D.; Smelyanski, L.; Gershoni, J. M. *Nucleic Acids Res.* **2001**, *29*, E50.
(60) Hong, M.; Jakes, K. *J. Biomol. NMR* **1999**, *14*, 71−4.
(61) Pines, A. *J. Chem. Phys.* **1972**, *56*, 1776.
(62) Metz, G.; Wu, X. L.; Smith, S. O. *J. Magn. Reson.* **1994**, *A110*, 219−227.
(63) Chandran, C. V.; Madhu, P. K.; Kurur, N. D.; Brauniger, T. *Magn. Reson. Chem.* **2008**, *46*, 943−947.
(64) Morcombe, C. R.; Gaponenko, V.; Byrd, R. A.; Zilm, K. W. *J. Am. Chem. Soc.* **2004**, *126*, 7196−7.
(65) Takegoshi, K.; Nakamura, S.; Terao, T. *Chem. Phys. Lett.* **2001**, *344*, 631−637.
(66) Hou, G.; Yan, S.; Trébosc, J.; Amoureux, J.-P.; Polenova, T. *J. Magn. Reson.* **2013**, *232*, 18−30.
(67) Szeverenyi, N. M.; Sullivan, M. J.; Maciel, G. E. *J. Magn. Reson.* **1982**, *47*, 462−475.
(68) Schaefer, J.; McKay, R. A.; Stejskal, E. O. *J. Magn. Reson.* **1979**, *34*, 443.
(69) Delaglio, F.; Grzesiek, S.; Vuister, G. W.; Zhu, G.; Pfeifer, J.; Bax, A. *J. Biomol. NMR* **1995**, *6*, 277−293.
(70) Goddard, T. D.; Kneller, D. B. *SPARKY*; University of California: San Francisco, CA, 2004.
(71) Morcombe, C. R.; Zilm, K. W. *J. Magn. Reson.* **2003**, *162*, 479−486.
(72) McDermott, A. E.; Gu, Z. *Encycl. Nucl. Magn. Reson.* **1996**, 1137−1147.
(73) Hayashi, S.; Hayamizu, K. *Bull. Chem. Soc. Jpn.* **1989**, *62*, 2429−2430.
(74) Ulrich, E. L.; Akutsu, H.; Doreleijers, J. F.; Harano, Y.; Ioannidis, Y. E.; Lin, J.; Livny, M.; Mading, S.; Maziuk, D.; Miller, Z.; Nakatani, E.; Schulte, C. F.; Tolmie, D. E.; Kent Wenger, R.; Yao, H.; Markley, J. L. *Nucleic Acids Res.* **2008**, *36*, D402−408.
(75) Massiot, D.; Alonso, B.; Fayon, F.; Fredoueil, F.; Bujoli, B. *Solid State Sci.* **2001**, *3*, 11−16.
(76) Marion, D.; Wüthrich, K. *Biochem. Biophys. Res. Commun.* **1983**, *113*, 967−974.
(77) Maniukiewicz, W.; Kwiatkowski, W.; Blessing, R. H. *Acta Crystallogr., Sect. C: Cryst. Struct. Commun.* **1996**, *52*, 1736−1741.
(78) Borer, P. N.; LaPlante, S. R.; Zanatta, N.; Levy, G. C. *Nucleic Acids Res.* **1988**, *16*, 2323−2332.
(79) Fonville, J. M.; Swart, M.; Vokacova, Z.; Sychrovsky, V.; Sponer, J. E.; Sponer, J.; Hilbers, C. W.; Bickelhaupt, F. M.; Wijmenga, S. S. *Chem.—Eur. J.* **2012**, *18*, 12372−12387.
(80) Greene, K. L.; Wang, Y.; Live, D. *J. Biomol. NMR* **1995**, *5*, 333−338.
(81) Lam, S. L.; Chi, L. M. *Prog. Nucl. Magn. Reson. Spectrosc.* **2010**, *56*, 289−310.
(82) Malináková, K.; Novosadová, L.; Lahtinen, M.; Kolehmainen, E.; Brus, J.; Marek, R. *J. Phys. Chem. A* **2010**, *114*, 1985−95.
(83) Ghose, R.; Marino, J. P.; Wiberg, K. B.; Prestegard, J. H. *J. Am. Chem. Soc.* **1994**, *116*, 8827−8828.
(84) Santos, R. R. A.; Tang, P.; Harbison, G. G. S.; Biol, A. C. J. M.; Biol, W. J. M. *Biochemistry* **1989**, *28*, 9372−9378.
(85) Kwok, C. W.; Ho, C. N.; Chi, L. M.; Lam, S. L. *J. Magn. Reson.* **2004**, *166*, 11−18.
(86) Dejaegere, A. P.; Case, D. A. *J. Phys. Chem. A* **1998**, *5639*, 5280−5289.
(87) Xu, X.; Chiu, W. A. K.; Au-Yeung, S. C. F. *J. Am. Chem. Soc.* **1998**, *120*, 4230−4231.
(88) Farès, C.; Amata, I.; Carlomagno, T. *J. Am. Chem. Soc.* **2007**, 15814−15823.
(89) Laplante, S. R.; Boudreau, E. A.; Zanatta, N.; Levy, G. C.; Borer, P. N. *Biochemistry* **1988**, *27*, 7902−7909.
(90) Marzec, C. J.; Day, L. A. *Biophys. J.* **1988**, *53*, 425−440.
(91) Liu, D.; Day, L. *Science* **1994**, *265*, 671−674.
(92) Tsuboi, M.; Tsunoda, M.; Overman, S. A.; Benevides, J. M.; Thomas, G. J. *Biochemistry* **2010**, *49*, 1737−43.
(93) Wen, Z. Q.; Armstrong, A.; Thomas, G. J. *Biochemistry* **1999**, *38*, 3148−3156.
(94) Day, L. A.; Wiseman, R. L.; Marzec, C. J. *Nucleic Acids Res.* **1979**, *7*, 1393−1403.
(95) Purusottam, R. N.; Rai, R. K.; Sinha, N. *J. Phys. Chem. B* **2013**, *117*, 2837−2840.